

## IPHAS J062746.41+014811.3: a deeply eclipsing intermediate polar

A. Aungwerojwit<sup>1,2</sup>, B.T. Gänsicke<sup>3</sup>, P.J. Wheatley<sup>3</sup>, S.Pyrzas<sup>3</sup>, B. Staels<sup>4</sup>, T. Krajci<sup>5</sup>, and P. Rodríguez-Gil<sup>6,7,8</sup>

Received \_\_\_\_\_; accepted \_\_\_\_\_

---

<sup>1</sup>Department of Physics, Faculty of Science, Naresuan University, Phitsanulok, 65000, Thailand

<sup>2</sup>ThEP Centre, CHE, 328 Si Ayutthaya Road, Bangkok, 10400, Thailand

<sup>3</sup>Department of Physics, University of Warwick, Coventry CV4 7AL, UK

<sup>4</sup>CBA Flanders, Alan Guth Observatory, Koningshofbaan 51, Hofstade, Aalst, Belgium

<sup>5</sup>Astrokolhoz Observatory, 1351 Cloudcroft, NM 88317, USA

<sup>6</sup>Instituto de Astrofísica de de Canarias, Vía Láctea, s/n, La Laguna, E-38205, Tenerife, Spain

<sup>7</sup>Departamento de Astrofísica de, Universidad de La Laguna, Avda. Astrofísico Fco. Sánchez, sn, La Laguna, E-38206, Tenerife, Spain

<sup>8</sup>Isaac Newton Group of Telescopes, Apartado de correos 321, S/C de la Palma, E-38700, Canary Islands, Spain

## ABSTRACT

We present time-resolved photometry of a cataclysmic variable discovered in the Isaac Newton Telescope Photometric H $\alpha$  Survey of the northern galactic plane, IPHAS J062746.41+014811.3 and classify the system as the fourth deeply eclipsing intermediate polar known with an orbital period of  $P_{\text{orb}} = 8.16$  h, and a spin period of  $P_{\text{spin}} = 2210$  s. The system shows mild variations of its brightness, that appear to be accompanied by a change in the amplitude of the spin modulation at optical wavelengths, and a change in the morphology of the eclipse profile. The inferred magnetic moment of the white dwarf is  $\mu_{\text{wd}} \sim 6-7 \times 10^{33}$  G cm<sup>3</sup>, and in this case IPHAS J0627 will either evolve into a short-period EX Hya-like intermediate polar with a large  $P_{\text{spin}}/P_{\text{orb}}$  ratio, or, perhaps more likely, into a synchronised polar. *Swift* observations show that the system is an ultraviolet and X-ray source, with a hard X-ray spectrum that is consistent with those seen in other intermediate polars. The ultraviolet light curve shows orbital modulation and an eclipse, while the low signal-to-noise ratio X-ray light curve does not show a significant modulation on the spin period. The measured X-ray flux is about an order of magnitude lower than would be expected from scaling by the optical fluxes of well-known X-ray selected intermediate polars.

*Subject headings:* stars: individual (IPHAS J062746.41+014811.3) – cataclysmic variables, intermediate polar, eclipsing

## 1. Introduction

Cataclysmic variables (CVs) are semi-detached close binary systems comprising an accreting white dwarf, and a late-type main-sequence donor. The strength of the magnetic field of the white dwarf plays an important role in governing the process of accretion. If the magnetic field is weak, mass transfer takes place via an accretion disk. In contrast, if the magnetic field is strong enough ( $B \sim 10\text{--}200$  MG) to suppress the formation of the disk, the accretion stream from the secondary star flows along the magnetic field lines to the poles of the white dwarf. These systems are known as polars. For moderate magnetic-field strength systems ( $B \sim 1\text{--}10$  MG), or intermediate polars (IPs), the transferred material may form a partial disk in which the inner part is disrupted into accretion curtains that channel material to the magnetic poles of the white dwarf. In polars, the rotational period of the white dwarf ( $P_{\text{spin}}$ ) is generally synchronised to the orbital period ( $P_{\text{orb}}$ ), whereas the white dwarfs in IPs are rotating asynchronously with  $P_{\text{spin}}/P_{\text{orb}} \sim 0.01\text{--}0.6$  (see Warner 1995 for a comprehensive review on CVs).

The evolution of magnetic CVs is still subject to discussion. Observationally, polars and IPs dominate the population of magnetic CVs below and above the 2–3 h orbital period gap, respectively. Both classes overlap in magnetic field strength, suggesting that IPs with relatively high fields may synchronise once they have evolved through the period gap, and appear as polars (e.g. Hellier 2001; Cumming 2002). IPs with low field strengths should remain unsynchronised below the period gap. This general hypothesis has been backed by the detailed simulations of Norton et al. (2004), who find that long-period IPs with a white dwarf magnetic moment of  $\mu_{\text{wd}} \gtrsim 5 \times 10^{33} \text{ G cm}^3$  will evolve into polars while those with  $\mu_{\text{wd}} \lesssim 5 \times 10^{33} \text{ G cm}^3$  and secondary stars with weak magnetic fields will remain IPs. Historically, the dearth of known IPs below the period gap has raised some concerns regarding the evolution of low-field IPs, however, a number of such systems have been identified (see e.g. Rodríguez-Gil et al. 2004a; Patterson et al. 2004; Southworth et al. 2007a), suggesting that their number has been underestimated.

We are currently investigating the population of CVs within the galactic plane, making use of the Isaac Newton Telescope (INT)/Wide Field Camera (WFC) Photometric H $\alpha$  Survey of the northern galactic plane (IPHAS, Drew et al. 2005; González-Solares et al. 2008). Witham et al. (2007) presented the first eleven new CVs identified within IPHAS because of their H $\alpha$  emission. Here, we present follow-up time-resolved photometry of the eclipsing CV, IPHAS J062746.41+014811.3 (hereafter IPHAS J0627), suggested by Witham et al. (2007) to be a long-period system, and classify it as the fourth deeply eclipsing IP, making it a promising candidate for accurate stellar parameter measurements. Following the determination of the orbital and spin periods of IPHAS J0627, along with estimates of its binary inclination and mass ratio, we discuss the sample of confirmed IPs as well as the future evolution of IPHAS J0627.

## 2. Observations and data reduction

### 2.1. Time-series photometry

We obtained a total of  $\sim 27$  h of unfiltered time-series CCD differential photometry of IPHAS J0627 (Fig. 1) during the period December 2006 and October 2007 at the Roque de los Muchachos Observatory on La Palma using the 1.2 m Mercator telescope equipped with the  $2k \times 2k$  pixel MEROPE CCD camera (Table 1). The images were taken using  $3 \times 3$  binning to reduce the read-out noise and to improve the time resolution. The data were reduced using the pipeline described by Gänsicke et al. (2004) which employs MIDAS for bias subtraction and flat fielding, and performs aperture photometry using *SExtractor* (Bertin & Arnouts 1996). Differential magnitudes of IPHAS J0627 were then calculated relative to the comparison star C1 (USNO-A2.0 0900-02977965:  $R=16.1$ ,  $B=18.0$ ). C2 (USNO-A2.0 0900-02978083:  $R=17.1$ ,  $B=18.1$ ) was used to check for variability of C1 which no significant brightness changes were found. Sample light curves of IPHAS J0627 are shown in Fig. 2.

One additional light curve of IPHAS J0627 was obtained quasi-simultaneous with the *Swift* X-ray observations (see below) using the AAVSONet telescope Wright28, a C-11 equipped with an ST-7 camera. The data were reduced in a standard fashion using MaximDL/CCD.

## **2.2. *Swift* X-ray and ultraviolet data**

IPHAS J0627 was observed with the narrow-field instruments of the *Swift* spacecraft (Gehrels et al. 2004) for a total of 9 ks on 23 November 2009. The observation was broken across nine spacecraft orbits, with exposure times ranging from 0.2 to 1.5 ks.

Observations with the Ultraviolet/Optical Telescope (UVOT; Roming et al. 2005) were made using the UVM2 filter, which has central wavelength of 217 nm and a full-width at half-maximum bandwidth of 51 nm. One exposure was made each visit. A source was visible at the position of IPHAS J0627 in all nine images, and a light curve was extracted from a 5 arcsec radius region using the UVOTMAGHIST tool version 1.12 and photometric calibration data from the release of 22 May 2007 (version 105).

Observations with the X-ray Telescope (XRT; Burrows et al. 2005) were made predominantly in photon counting mode (PC) and we did not attempt to analyse the 10 per cent of data collected in Windowed Timing mode (WT). A light curve and spectrum were extracted within a 20 pixel (47 arcsec) radius circle of the source position from the cleaned event file using XSELECT version 2.4 and retaining events with grades 0–12. The background was estimated using a circular region of 4.6′ radius. The spectrum was binned to a minimum of five counts per bin.

### 3. Light curve analysis

The light curves in Fig. 2 confirm the deeply eclipsing nature of IPHAS J0627 found by Witham et al. (2007). In addition, the 2006 data exhibit two additional features: short-period modulation and a broad modulation of the out-of-eclipse brightness of the system. Below, we analyse these three morphological light curve structures.

#### 3.1. Eclipse profiles and ephemeris

Witham et al. (2007) used two accurate eclipse times plus a rough estimate of a third eclipse time to determine a set of four possible orbital periods for IPHAS J0627,  $\sim 1.02$  d,  $\sim 0.51$  d,  $\sim 0.34$  d and  $\sim 0.25$  d. One aim of the observations discussed here was to measure the actual orbital period of IPHAS J0627 and to determine an accurate eclipse ephemeris. For that purpose, we determined mid-eclipse times by mirroring and shifting the eclipse profiles until the best match in overall shape was achieved. Combining these six new eclipse times (Table 2) with those from Witham et al. (2007), we determined a unique cycle count and a best-fit linear ephemeris

$$T_0 = \text{HJD}2453340.50732(40) + 0.34008253(14) \times E \quad (1)$$

where  $T_0$  is defined as the time of mid-eclipse and the errors are given in brackets. We hence conclude that the orbital period of IPHAS J0627 is  $P_{\text{orb}} = 8.1619807(34)$  h. The corresponding cycle numbers and observed minus computed (O–C) eclipse times are reported in Table 2.

The Mercator light curves folded on the ephemeris in Eq. (1) are shown in Fig. 3, illustrating a noticeable change in the shape of the eclipse profiles. The two light curves obtained on 2006 December 22 & 23 show nearly perfect agreement, with a relatively round-shaped bottom of the eclipse profile, whereas the 2007 observations exhibit nightly variation in the eclipse profile, and are overall more box-shaped. In 2006, the eclipse depth of the average light curve was  $\simeq 1.3 \pm 0.1$  mag, and the full-width of the eclipse at half depth was  $\Delta\phi_{1/2} \simeq 0.115 \pm 0.006$  (see

Sect. 4 for details of estimating  $\Delta\phi_{1/2}$ ). In 2007, the eclipse depth was  $\sim 1.43 \pm 0.05$  mag, with a full-width at half depth of  $\Delta\phi_{1/2} \simeq 0.106 \pm 0.002$ . The 2009 observations were taken with very long exposure times, but at face value, the eclipse had a similar round-shaped profile as in 2006.

In addition to the change in the eclipse profile morphology, we investigated the out-of-eclipse brightness variations by measuring the average magnitude in the phase interval 0.8–0.9 and 1.1–1.2. These measurements suggest that the out-of-eclipse magnitude of IPHAS J0627 is varying by  $\sim 0.2$  mag, with the system having been found at  $\simeq 16.3$  mag,  $\simeq 16.5$  mag, and  $\simeq 16.3$  mag in 2006, 2007, and 2009, respectively. The decreased brightness level and the narrower eclipse width observed in 2007 imply that the accretion disk contributed less to the optical light during that epoch. The flat bottom of the eclipse profile is suggestive that the white dwarf and the accretion disk may have been totally eclipsed, a higher time resolution study could potentially resolve the white dwarf ingress and egress.

### 3.2. Spin modulation

In addition to the deep eclipses, the December 2006 light curves of IPHAS J0627 exhibit short-period modulation on time-scales of  $\sim 40$  min with a  $\sim 0.4$ – $0.5$  mag peak-to-peak amplitude, most clearly seen in the December 23 observations covering more than one orbital cycle (see Fig. 2). Considering the detection of He II  $\lambda 4686$  emission in the spectrum of IPHAS J0627 (Witham et al. 2007), this raises the possibility that the observed oscillations represent the white dwarf spin period.

In order to test the periodicity of the oscillations, we subjected the combined light curves 2006 December 22 and 23 observations to a time-series analysis using the MIDAS/TSA context. Prior to the analysis, the mean was subtracted from the data. In addition, we pre-whitened the data by means of a sine fit, fixing the period of the sine wave to the orbital. We included nine harmonic

frequencies in the sine fit to remove the effect of the eclipse from the observed light curve.

The power spectrum computed from the data prepared in this way contains the strongest signal at  $f_1 = 39.090(15) \text{ d}^{-1}$  (Fig. 4), flanked by one-day aliases. The best-fit value of the period determined from a sine fit to the data is  $2210.27(87) \text{ s}$ . We assessed the likelihood of correct alias choice using a test based on bootstrapping simulations as described in Southworth et al. (2006, 2007b), and find that 100% of the simulations return the strongest power within the  $39.090 \text{ d}^{-1}$  alias. We tested the significance of this signal by creating a faked data set computed from a sine function with a frequency of  $39.090 \text{ d}^{-1}$ , and randomly offset from the computed sine wave using the observed errors. The power spectrum of the faked data set reproduces well the 1-day alias structure of the power spectrum calculated from the observations of IPHAS J0627 (Fig. 4, *top curve*). The photometric data folded on  $2210 \text{ s}$  display a quasi-sinusoidal modulation with an amplitude of  $\sim 0.2 \text{ mag}$  (Fig. 5). Such coherent and large-amplitude optical modulation is a hallmark of intermediate polars, e.g. FO Aqr (Patterson et al. 1998), AO Psc (Patterson & Price 1981), or MU Cam (Araujo-Betancor et al. 2003). Typically, the power spectra of IPs show signals at the orbital frequency,  $\Omega$ , the white dwarf spin frequency,  $\omega$ , and the orbital side-bands  $\omega \pm \Omega$  and  $\omega - 2\Omega$  (e.g. Warner 1986). Inspecting the power spectrum in the top panel of Fig. 4 reveals power in excess of the alias structure. The strongest signal in the power spectrum computed from the data pre-whitened with  $f_1 = 39.090 \text{ d}^{-1}$  (Fig. 4, second panel from top) is found at  $f_2 = 33.244(29) \text{ d}^{-1}$  which is, within the uncertainties, equal to  $f_1 - 2\Omega$ . Additional low-amplitude signals are seen near  $f_1 + 2\Omega$  and possibly  $2(f_1 - \Omega)$ , however, longer time-series photometry will be necessary to confirm the presence of these signals. Based on the most commonly observed behaviour among the known IPs, we identify the strongest signal as the white dwarf spin frequency,  $\omega = f_1$ , and the weaker signal as an orbital side-band  $\omega - 2\Omega$ . Alternatively,  $f_2$  is the spin frequency, in which case the strongest signal would be the  $\omega + 2\Omega$  side-band, however, we consider this option less likely. We hence conclude that IPHAS J0627 is an eclipsing intermediate polar, and the white dwarf spin period is most likely  $P_{\text{spin}} = 2210.27(87) \text{ s}$ , where the error was determined by means of a sine fit



to the spin light curve.

The amplitude of the optical spin modulation undergoes large long-term variations, as it was very weak in our short observations in October 2007 (see Fig. 4, third panel from top). The weakening of the spin signal in 2007 may have been caused by a lower accretion rate, as suggested by the fainter magnitude compared to the 2006 observations. In 2009, when the system was again brighter, the spin modulation was back, though with a lower amplitude compared to 2006 (Fig. 4, bottom panel). The spin period determined from that single night was found to be 2237(10) sec. Pre-whitening the light curve with a multi-harmonic sine-fit to remove the effect of the eclipse introduces a systematic uncertainty into measurement of the spin period, and we conclude that the 2006 and 2009 values of the spin period are broadly consistent with each other.

### 3.3. Orbital modulation: a reflection effect?

Another distinct feature found in the light curves of IPHAS J0627 is a broad modulation outside the eclipses, detected in the long observation on 2006 December 23. This modulation may be caused by a reflection effect, i.e. heating of the inner hemisphere of the donor star by the accreting white dwarf, such as observed in CVs (e.g. DD Cir; Woudt & Warner 2003) or in pre-CVs containing hot primary stars (e.g. HW Vir; Hilditch et al. 1996, or HS1857+5144; Aungwerojwit et al. 2007). We investigated this modulation by pre-whitening the 2006 December 23 with the spin period,  $P_{\text{spin}} = 2210$  s, and folding the data over the orbital period,  $P_{\text{orb}} = 8.16$  h. The 2007 October 14–16 light curves are combined and folded on the orbital period. Phase-folded light curves are shown in Fig. 6 with a maximum brightness at  $\phi \simeq 0.5$  which is in agreement with maximum light at superior conjunction of the secondary star when taken reflection effect into account. Fitting a sine wave to the modulation outside the eclipse, we find the amplitude of the modulation to be  $\sim 0.14$  mag and  $\sim 0.33$  mag for the 2006 and 2007 light curves, respectively. Based on our limited data, we suggest that the larger amplitude of the modulation observed in

2007 may be related with the fainter accretion disk contributing somewhat less to the optical light. In order to confirm our hypothesis, long-term observations covering the entire orbital period are strongly encouraged.

#### 4. Orbital inclination

Considering the geometry of a point eclipse by a spherical body, we estimated the inclination,  $i$ , of a binary system through the relation

$$\left(\frac{R_2}{a}\right)^2 = \sin^2(\pi\Delta\phi_{1/2}) + \cos^2(\pi\Delta\phi_{1/2})\cos^2 i, \quad (2)$$

where  $R_2/a$  is the volume radius of the secondary star, which depends only on the mass ratio,  $q = M_2/M_1$  (Eggleton 1983):

$$\left(\frac{R_2}{a}\right) = \frac{0.49q^{2/3}}{0.6q^{2/3} + \ln(1+q^{1/3})} \quad (3)$$

and  $\Delta\phi_{1/2}$  is the full-width of eclipse at half depth (see also e.g. Dhillon et al. 1991; Rodríguez-Gil et al. 2004b). We estimated  $\Delta\phi_{1/2}$  for IPHAS J0627 from the 2006, 2007, and 2009 combined light curves with an average out-of-eclipse magnitude of  $16.5 \pm 0.1$ ,  $16.7 \pm 0.1$ , and  $16.6 \pm 0.1$ , respectively. This yields  $\Delta\phi_{1/2} \simeq 0.115 \pm 0.006$ ,  $\Delta\phi_{1/2} \simeq 0.106 \pm 0.002$ , and  $\Delta\phi_{1/2} \simeq 0.120 \pm 0.005$  for 2006, 2007, and 2009 observations, respectively; the large error is due to the large uncertainty in identifying the out-of-eclipse brightness.

In order to obtain the inclination of the system, a given value of the mass ratio,  $q$ , need to be assumed. Using the mean empirical mass-period relation of Smith & Dhillon (1998),

$$\frac{M_2}{M_\odot} = (0.126 \pm 0.011)P_{\text{orb}} - (0.11 \pm 0.04) \quad (4)$$

where  $P_{\text{orb}}$  is expressed in hours, we find  $0.87M_\odot \lesssim M_2 \lesssim 0.97M_\odot$  for the secondary star in IPHAS J0627. Ramsay (2000) estimated a mean value of  $M_1 = 0.85 \pm 0.21 M_\odot$  for the white dwarf

mass in intermediate polars, which is broadly consistent with the mean white dwarf mass across all CVs (Knigge 2006; Littlefair et al. 2008; Knigge et al. 2011; Zorotovic et al. 2011). Assuming stable mass transfer, we adopt  $0.85 M_{\odot} \lesssim M_1 \lesssim 1.06 M_{\odot}$ , resulting in  $0.8 \lesssim q \lesssim 1.0$ . This finally leads to an orbital inclination of  $77^{\circ} \lesssim i \lesssim 84^{\circ}$  which is in a good agreement with the values derived in term of graphical form of the relationship between  $\Delta\phi_{1/2}$ ,  $i$ , and  $q$  for Roche geometry in Horne (1985).

## 5. The *Swift* observations

A faint X-ray source was detected at the position of IPHAS J0627 with a count rate of  $3.2 \pm 0.7 \text{ ks}^{-1}$ . The X-ray spectrum is plotted in Fig. 7 compared with the best-fitting optically-thin thermal plasma model (Mewe et al. 1986; Liedahl et al. 1995). In this fit, the temperature has risen to the model maximum of 80 keV, and it is clear that the observed spectrum is harder still. The fit is only marginally acceptable with a reduced  $\chi^2$  of 1.75 with 4 degrees of freedom. Adding a cold absorber to the model improves the fit to a reduced  $\chi^2$  of 1.30 (3 degrees of freedom) with a best-fitting  $N_{\text{H}}$  of  $5 \times 10^{21} \text{ cm}^{-2}$ . The hard spectrum and high absorption are as expected for an intermediate polar, but since the source is located close to the Galactic Plane it is not clear whether this absorption is intrinsic or interstellar. The total Galactic column in the direction of IPHAS J0627 is also  $5 \times 10^{21} \text{ cm}^{-2}$ . However, the fit is further improved by allowing the absorber to only partially cover the source, with a higher column density of  $N_{\text{H}} = 4 \times 10^{22} \text{ cm}^{-2}$ , a partial-covering fraction of 0.9, and a temperature that is no longer forced the highest allowed values,  $kT = 5 \text{ keV}$ . This fit yields a reduced  $\chi^2$  of 0.96 with 2 degrees of freedom. Although the signal to noise ratio is low, we can conclude that the X-ray spectrum of IPHAS J0627 is consistent with that expected for an intermediate polar. The 0.5–10 keV flux of the best-fitting model is  $2.2 \times 10^{-13} \text{ erg s}^{-1} \text{ cm}^{-2}$ . This is about an order of magnitude fainter than would be expected from scaling by the optical fluxes of well studied (and usually X-ray selected) IPs (e.g. Landi et al.

2009; Brunschweiler et al. 2009; Scaringi et al. 2010).

In order to search for the presence of a white-dwarf spin modulation in the X-ray data we folded the XRT light on the period of 2210 s. The folded light curve is presented in Fig. 5 (bottom panel) and does not show any sign of a modulation at this period. However, with such a low number of events detected, the 90 per cent confidence upper limit on the amplitude of a sinusoidal modulation is 65 per cent. So the *Swift* data do not rule out the presence of an X-ray spin modulation in this object. A Fourier analysis of the X-ray light curve also failed to reveal any other significant periods.

The *Swift* ultraviolet data were obtained in the imaging mode, i.e. no time information is available for individual photons, but only average ultraviolet fluxes for each of the nine spacecraft orbits. The one ultraviolet measurement made close to the optical eclipse phase also has the lowest flux, indicating that the eclipse is also present at ultraviolet wavelengths. Excluding the eclipse, the ultraviolet flux at 217 nm varies in the range  $5\text{--}13 \times 10^{-17} \text{ erg s}^{-1} \text{ cm}^{-2}$ , exceeding the statistical errors on the flux individual measurements.

## 6. Discussion

Over the past few years, the number of confirmed intermediate polars has rapidly increased. At the time of writing, the IP page by K. Mukai<sup>1</sup> lists 36 confirmed IPs while Ritter & Kolb (2003, v.7.12) contains roughly twice this number, which underlines the rather broad range of criteria adopted by different authors to classify a system as IP. One clear hallmark of IPs is the presence of coherent optical and/or X-ray short-term variability on the white dwarf spin period over a sufficient span of time (e.g. Buckley 2000).

---

<sup>1</sup><http://asd.gsfc.nasa.gov/Koji.Mukai/iphome/iphome.html>

Detailed measurements of the physical parameters of CVs come from observational studies of eclipsing systems. Mukai’s IP list contains only six confirmed eclipsing IPs, of which four only show grazing/partial eclipses: FO Aqr (e.g. Hellier et al. 1990; Kruszewski & Semeniuk 1993), BG CMi (e.g. Patterson & Thomas 1993; Kim et al. 2005), TV Col (e.g. Hellier et al. 1991; Hellier 1993), EX Hya (e.g. Beuermann & Osborne 1988). The other two, DQ Her (e.g. Walker 1954, 1956) and XY Ari (Patterson & Halpern 1990) are deeply eclipsing IPs. Detailed observational and theoretical studies of DQ Her provided tight constraints on its system parameters, i.e.  $P_{\text{orb}}$ ,  $\Delta\phi_{1/2}$ ,  $q$ ,  $i$ ,  $M_1$ ,  $M_2$ , and disk radius (see e.g. Horne et al. 1993; Zhang et al. 1995). XY Ari exhibits deep X-ray eclipses, but is hidden behind the molecular cloud MBM12 which makes it virtually invisible in the optical band (Littlefair et al. 2001). Recently, Warner & Woudt (2009) identified V597 Pup as a third deeply eclipsing ( $\simeq 1$  mag depth) IP, which is in the stage of decline to its pre-eruption brightness at  $V \sim 20$ .

Based on the optical short-period variation at  $P_{\text{spin}} = 2210$  s detected in our 2006 light curves, we classify IPHAS J0627 as the fourth deeply eclipsing IP with  $P_{\text{orb}} = 8.16$  h, turning it to a rare object that holds substantial promises for detailed optical and X-ray follow-up studies.

We adopted Mukai’s conservative classification, and updated his list with additional 9 IPs: V597 Pup, IGR J16500-3307, IGR J17195-4100, IGR J19267+1325, 1RXS J165443.5-191620, IGR J08390-4833, IGR J18308-1232, IGR J18173-2509, IPHAS J0627, and 3 IPs from Fig. 23 of Gänsicke et al. (2005) i.e., RXJ0153.3+7446, HS 0943+1404, 1RXS J063631.9+353537. Figure 8 shows the most up-to-date distribution of the 48 confirmed IPs in the  $P_{\text{spin}} - P_{\text{orb}}$  plane (updated with respect to Fig. 23 of Gänsicke et al. (2005) and with the additional well-determined  $P_{\text{orb}}$  and  $P_{\text{spin}}$  IPs listed in Table 3). Eclipsing systems presented as filled dots. It is clear that the majority of IPs ( $\sim 87\%$ ) are found above the conventional 2–3 h period gap whilst the fraction of systems below the period gap remains fairly small ( $\sim 13\%$ ). Only two systems have extremely long orbital periods i.e., GK Per ( $P_{\text{orb}} = 1.996$  d; Crampton et al. 1986) and 1RXS J173021.5-055933

( $P_{\text{orb}} = 15.42$  h; Gänsicke et al. 2005).

The updated distribution shows that a fair number of CVs have  $P_{\text{spin}}/P_{\text{orb}} \simeq 0.1$ , a trend already noticed frequently in the past (e.g. Barrett et al. 1988; Norton et al. 2004; Gänsicke et al. 2005; Scaringi et al. 2010), which spawned the initial theoretical work on the white dwarf equilibrium in magnetic CVs (King & Lasota 1991; Warner & Wickramasinghe 1991). However, it is now clear that IPs above the period gap (3–10 h) are widely distributed over  $0.01 \lesssim P_{\text{spin}}/P_{\text{orb}} \lesssim 0.1$ , including IPHAS J0627 with  $P_{\text{spin}}/P_{\text{orb}} = 0.075$  (for the adopted  $P_{\text{spin}} = 2210$  s), indicating disk-fed accretion (Norton et al. 2004, 2008). All IPs with  $P_{\text{orb}} < 2$  h have  $P_{\text{spin}}/P_{\text{orb}} > 0.1$  which agrees with the predictions of King & Wynn (1999). The most extreme systems with  $P_{\text{spin}}/P_{\text{orb}} < 0.01$  are exclusively found at very long orbital periods, which may suggest that they are relatively young systems still far from equilibrium.

Norton et al. (2004) showed that a large range of spin equilibria exists in the  $(P_{\text{spin}}/P_{\text{orb}}, P_{\text{orb}}, \mu_{\text{wd}}, q)$  parameter plane, with  $\mu_{\text{wd}}$  being the magnetic moment of the white dwarf, as illustrated for a mass ratio  $q = 0.5$  in their Fig. 2. For  $P_{\text{orb}} = 8.16$  h,  $P_{\text{spin}}/P_{\text{orb}} = 0.075$  (adopting a spin period of 2210 s), and correcting for the higher mass ratio of IPHAS J0627 ( $q \simeq 0.8$ , see Eq. 11 of Norton et al. 2004), we estimate from the Fig. 2  $\mu_{\text{wd}} \sim 6-7 \times 10^{33}$  G cm<sup>3</sup>. With such a relatively high magnetic moment, IPHAS J0627 may just about evolve into a short-period EX Hya-like IP, with a large  $P_{\text{spin}}/P_{\text{orb}}$  ratio, or, perhaps more likely, synchronise as a polar. In fact, adopting  $R_{\text{wd}} = 0.01 R_{\odot}$  (appropriate for the average CV white dwarf mass of  $0.85 M_{\odot}$ ), the estimated magnetic moment implies a field strength of  $B \simeq 18$  MG, which comparable to that of the short-period polars EF Eri and ST LMi.

The motivation of our *Swift* observation of IPHAS J0627 was to probe for X-ray emission pulsed on the white dwarf spin period, which would be the ultimate confirmation of the IP nature of this system. We found that the best-fitting model at 0.5–10 keV flux for IPHAS J0625 is  $2.2 \times 10^{-13}$  erg s<sup>-1</sup> cm<sup>-2</sup>. This value is an order of magnitude fainter than most confirmed IPs

which usually are X-ray selected. Figure 9 presents X-ray fluxes and optical magnitudes of the confirmed IPs<sup>2</sup>, and optical magnitudes were taken from Ritter & Kolb (2003, v.7.12), with filled dots represented eclipsing systems, triangles being rapid rotators ( $P_{\text{spin}}/P_{\text{orb}} < 0.01$ ), and filled triangles being eclipsing and rapid rotators. IPHAS J0627 has clearly the lowest X-ray-to-optical flux ratio, followed by DQ Her and AE Aqr. The low X-ray flux in AE Aqr is explained by the very rapid rotation of the white dwarf, which prevents accretion (Wynn et al. 1997). Among the other two rapid rotators, DQ Her has a low X-ray flux, but 1RXSJ173021.5-055933 is X-ray bright – both have spin periods 3–4 times longer than AE Aqr, suggesting that inefficient accretion is not necessarily the reason for the low X-ray flux of DQ Her. The other plausible hypothesis is that the X-ray flux in DQ Her is blocked by the accretion disk/rim because of the high binary inclination ( $i = 86.5^\circ$ , Horne et al. 1993). To complicate the matters, XY Ari is a deeply eclipsing ( $i < 84^\circ$ , Hellier 1997), but X-ray bright IP. However, it is difficult to assess an ‘intrinsic’ X-ray-flux-to-optical ratio for XY Ari since the system lies behind the molecular cloud MBM12. For partial/grazing eclipsing IPs, X-ray fluxes are typically consistent with non-eclipsing systems.

We conclude that the dependence of the X-ray-to-optical flux ratio on the binary inclination and white dwarf spin is not straight-forward, but for the case of IPHAS J0627 obscuration of the accretion spots on the white dwarf by the accretion disk/rim appears to be the most likely explanation for the low X-ray flux. High-speed ground-based photometry of IPHAS J0627 has the potential to settle the question whether or not the white dwarf is hidden from direct view.

---

<sup>2</sup>All X-ray fluxes used in Fig. 9 were taken from Mukai’s list with 2-10 keV fluxes except DQ Her (Patterson 1994), 1RXSJ070407.9+262501 (Anzolin et al. 2008), MUCam (=IGR J06253+7334), 1RXSJ173021.5-055933 (=IGR J17303-0601), IGR J16500-3307, IGR J17195-4100, V2069-Cyg (Landi et al. 2009), IGR J00234+6141 (Anzolin et al. 2009), IGR J08390-4833, IGR J18308-1232, IGR J18173-2509 (Bernardini et al. 2012)

## 7. Conclusions

We have identified IPHAS J0627.41+014811.3 as the fourth deep eclipsing IP with an orbital period of  $P_{\text{orb}} = 8.1619807(34)$  h, and a spin period of  $P_{\text{spin}} = 2210.27(87)$  s. Because of its eclipsing nature, this IP is particularly well suited for detailed follow-up studies that will provide detailed and accurate insight into the system parameters. Our photometric data spanning three observing seasons reveal variations in the system brightness, the amplitude of the optical spin modulation, and the morphology of the eclipse profiles, all of which can tentatively be explained by a variation in the accretion rate. The relatively large magnetic moment of the white dwarf in IPHAS J0627 suggests that it is right at the boundary of systems evolving into either short-period EX Hya IPs or synchronised polars.

This work is supported by the Thailand Research Fund under grant number MRG5180136. We gratefully acknowledge the observations of IPHAS J0627 taken through AAVSOnet, operated by the American Association of Variable Star Observers. We thank the referee for his/her constructive comments which have improved the paper.

*Facilities:* Mercator1.2m, Swift, AAVSO



## REFERENCES

- Anzolin, G., de Martino, D., Bonnet-Bidaud, J.-M., Mouchet, M., Gänsicke, B. T., Matt, G., & Mukai, K. 2008, *aa*, 489, 1243
- Anzolin, G., de Martino, D., Falanga, M., Mukai, K., Bonnet-Bidaud, J.-M., Mouchet, M., Terada, Y., & Ishida, M. 2009, *aa*, 501, 1047
- Araujo-Betancor, S., Gänsicke, B. T., Hagen, H.-J., Rodríguez-Gil, P., & Engels, D. 2003, *A&A*, 406, 213
- Aungwerojwit, A., Gänsicke, B. T., Rodríguez-Gil, P., Hagen, H.-J., Giannakis, O., Papadimitriou, C., Allende Prieto, C., & Engels, D. 2007, *A&A*, 469, 297
- Barrett, P., O’Donoghue, D., & Warner, B. 1988, *MNRAS*, 233, 759
- Bernardini, F., de Martino, D., Falanga, M., Mukai, K., Matt, G., Bonnet-Bidaud, J.-M., Masetti, N., & Mouchet, M. 2012, *A&A*, 542, A22
- Bertin, E. & Arnouts, S. 1996, *A&AS*, 117, 393
- Beuermann, K. & Osborne, J. P. 1988, *A&A*, 189, 128
- Bonnet-Bidaud, J. M., de Martino, D., Falanga, M., Mouchet, M., & Masetti, N. 2007, *A&A*, 473, 185
- Bonnet-Bidaud, J. M., de Martino, D., & Mouchet, M. 2009, *The Astronomer’s Telegram*, 1895, 1
- Bonnet-Bidaud, J. M., Mouchet, M., de Martino, D., Silvotti, R., & Motch, C. 2006, *A&A*, 445, 1037
- Brunschweiler, J., Greiner, J., Ajello, M., & Osborne, J. 2009, *aa*, 496, 121
- Buckley, D. A. H. 2000, *New Astronomy*, 44, 63

- Burrows, D. N., Hill, J. E., Nousek, J. A., Kennea, J. A., Wells, A., Osborne, J. P., Abbey, A. F., Beardmore, A., Mukerjee, K., Short, A. D. T., Chincarini, G., Campana, S., Citterio, O., Moretti, A., Pagani, C., Tagliaferri, G., Giommi, P., Capalbi, M., Tamburelli, F., Angelini, L., Cusumano, G., Bräuninger, H. W., Burkert, W., & Hartner, G. D. 2005, *Space Science Reviews*, 120, 165
- Butters, O. W., Barlow, E. J., Norton, A. J., & Mukai, K. 2007, *A&A*, 475, L29
- Butters, O. W., Norton, A. J., Hakala, P., Mukai, K., & Barlow, E. J. 2008, *A&A*, 487, 271
- Crampton, D., Fisher, W. A., & Cowley, A. P. 1986, *ApJ*, 300, 788
- Cumming, A. 2002, *MNRAS*, 333, 589
- Dhillon, V. S., Marsh, T. R., & Jones, D. H. P. 1991, *MNRAS*, 252, 342
- Drew, J. E., Greimel, R., Irwin, M. J., Aungwerojwit, A., Barlow, M. J., Corradi, R. L. M., Drake, J. J., Gänsicke, B. T., Groot, P., Hales, A., Hopewell, E. C., Irwin, J., Knigge, C., Leisy, P., Lennon, D. J., Mampaso, A., Mashedier, M. R. W., Matsuura, M., Morales-Rueda, L., Morris, R. A. H., Parker, Q. A., Phillipps, S., Rodríguez-Gil, P., Roelofs, G., Skillen, I., Sokoloski, J. L., Steeghs, D., Unruh, Y. C., Viironen, K., Vink, J. S., Walton, N. A., Witham, A., Wright, N., Zijlstra, A. A., & Zurita, A. 2005, *MNRAS*, 362, 753
- Eggleton, P. P. 1983, *ApJ*, 268, 368
- Evans, P. A., Beardmore, A. P., & Osborne, J. P. 2008, *The Astronomer's Telegram*, 1669, 1
- Gänsicke, B. T., Araujo-Betancor, S., Hagen, H.-J., Harlaftis, E. T., Kitsionas, S., Dreizler, S., & Engels, D. 2004, *A&A*, 418, 265
- Gänsicke, B. T., Marsh, T. R., Edge, A., Rodríguez-Gil, P., Steeghs, D., Araujo-Betancor, S., Harlaftis, E., Giannakis, O., Pyrzas, S., Morales-Rueda, L., & Aungwerojwit, A. 2005, *MNRAS*, 361, 141

Gehrels, N., Chincarini, G., Giommi, P., Mason, K. O., Nousek, J. A., Wells, A. A., White, N. E., Barthelmy, S. D., Burrows, D. N., Cominsky, L. R., Hurley, K. C., Marshall, F. E., Mészáros, P., Roming, P. W. A., Angelini, L., Barbier, L. M., Belloni, T., Campana, S., Caraveo, P. A., Chester, M. M., Citterio, O., Cline, T. L., Cropper, M. S., Cummings, J. R., Dean, A. J., Feigelson, E. D., Fenimore, E. E., Frail, D. A., Fruchter, A. S., Garmire, G. P., Gendreau, K., Ghisellini, G., Greiner, J., Hill, J. E., Hunsberger, S. D., Krimm, H. A., Kulkarni, S. R., Kumar, P., Lebrun, F., Lloyd-Ronning, N. M., Markwardt, C. B., Mattson, B. J., Mushotzky, R. F., Norris, J. P., Osborne, J., Paczynski, B., Palmer, D. M., Park, H., Parsons, A. M., Paul, J., Rees, M. J., Reynolds, C. S., Rhoads, J. E., Sasseen, T. P., Schaefer, B. E., Short, A. T., Smale, A. P., Smith, I. A., Stella, L., Tagliaferri, G., Takahashi, T., Tashiro, M., Townsley, L. K., Tueller, J., Turner, M. J. L., Vietri, M., Voges, W., Ward, M. J., Willingale, R., Zerbi, F. M., & Zhang, W. W. 2004, *ApJ*, 611, 1005

González-Solares, E. A., Walton, N. A., Greimel, R., Drew, J. E., Irwin, M. J., Sale, S. E., Andrews, K., Aungwerojwit, A., Barlow, M. J., van den Besselaar, E., Corradi, R. L. M., Gänsicke, B. T., Groot, P. J., Hales, A. S., Hopewell, E. C., Hu, H., Irwin, J., Knigge, C., Lagadec, E., Leisy, P., Lewis, J. R., Mampaso, A., Matsuura, M., Moont, B., Morales-Rueda, L., Morris, R. A. H., Naylor, T., Parker, Q. A., Prema, P., Pyzas, S., Rixon, G. T., Rodríguez-Gil, P., Roelofs, G., Sabin, L., Skillen, I., Suso, J., Tata, R., Viironen, K., Vink, J. S., Witham, A., Wright, N. J., Zijlstra, A. A., Zurita, A., Drake, J., Fabregat, J., Lennon, D. J., Lucas, P. W., Martín, E. L., Phillipps, S., Steeghs, D., & Unruh, Y. C. 2008, *MNRAS*, 388, 89

Gotthelf, J. P. & Halpern, E. V. 2010, *The Astronomer's Telegram*, 2681, 1

Hellier, C. 1993, *MNRAS*, 264, 132

—. 1997, *MNRAS*, 291, 71

—. 2001, *Cataclysmic Variable Stars* (Springer)

Hellier, C., Mason, K. O., & Cropper, M. 1990, *MNRAS*, 242, 250

Hellier, C., Mason, K. O., & Mittaz, J. P. D. 1991, *MNRAS*, 248, 5P

Hilditch, R. W., Harries, T. J., & Hill, G. 1996, *MNRAS*, 279, 1380

Homer, L., Szkody, P., Henden, A., Chen, B., Schmidt, G. D., Fraser, O. J., & West, A. A. 2006, *AJ*, 132, 2743

Hong, J. S., van den Berg, M., Laycock, S., Grindlay, J. E., & Zhao, P. 2009, *ApJ*, 699, 1053

Horne, K. 1985, *MNRAS*, 213, 129

Horne, K., Welsh, W. F., & Wade, R. A. 1993, *ApJ*, 410, 357

Kim, Y. G., Andronov, I. L., Park, S. S., & Jeon, Y. 2005, *A&A*, 441, 663

King, A. R. & Lasota, J. P. 1991, *ApJ*, 378, 674

King, A. R. & Wynn, G. A. 1999, *MNRAS*, 310, 203

Knigge, C. 2006, *MNRAS*, 373, 484

Knigge, C., Baraffe, I., & Patterson, J. 2011, *ApJS*, 194, 28

Kruszewski, A. & Semeniuk, I. 1993, *Acta Astron.*, 43, 127

Landi, R., Bassani, L., Dean, A. J., Bird, A. J., Fiacchi, M., Bazzano, A., Nousek, J. A., & Osborne, J. P. 2009, *MNRAS*, 392, 630

Liedahl, D. A., Osterheld, A. L., & Goldstein, W. H. 1995, *ApJ Lett.*, 438, L115

Littlefair, S. P., Dhillon, V. S., & Marsh, T. R. 2001, *MNRAS*, 327, 669

- Littlefair, S. P., Dhillon, V. S., Marsh, T. R., Gänsicke, B. T., Southworth, J., Baraffe, I., Watson, C. A., & Copperwheat, C. 2008, MNRAS, 388, 1582
- Mewe, R., Lemen, J. R., & van den Oord, G. H. J. 1986, A&AS, 65, 511
- Norton, A. J., Butters, O. W., Parker, T. L., & Wynn, G. A. 2008, ApJ, 672, 524
- Norton, A. J., Wynn, G. A., & Somerscales, R. V. 2004, ApJ, 614, 349
- Patterson, J. 1994, PASP, 106, 209
- Patterson, J. & Halpern, J. P. 1990, ApJ, 361, 173
- Patterson, J., Kemp, J., Richman, H. R., Skillman, D. R., Vanmunster, T., Jensen, L., Buckley, D. A. H., O'Donoghue, D., & Kramer, R. 1998, PASP, 110, 415
- Patterson, J. & Price, C. M. 1981, ApJ Lett., 243, L83
- Patterson, J. & Thomas, G. 1993, PASP, 105, 59
- Patterson, J., Thorstensen, J. R., Vanmunster, T., Fried, R. E., Martin, B., Campbell, T., Robertson, J., Kemp, J., Messier, D., & Armstrong, E. 2004, PASP, 116, 516
- Pretorius, M. L. 2009, MNRAS, 395, 386
- Ramsay, G. 2000, MNRAS, 314, 403
- Ramsay, G., Wheatley, P. J., Norton, A. J., Hakala, P., & Baskill, D. 2008, MNRAS, 387, 1157
- Reimer, T. W., Welsh, W. F., Mukai, K., & Ringwald, F. A. 2008, ApJ, 678, 376
- Ritter, H. & Kolb, U. 2003, A&A, 404, 301
- Rodríguez-Gil, P., Gänsicke, B. T., Araujo-Betancor, S., & Casares, J. 2004a, MNRAS, 349, 367
- Rodríguez-Gil, P., Gänsicke, B. T., Barwig, H., Hagen, H.-J., & Engels, D. 2004b, A&A, 424, 647

- Roming, P. W. A., Kennedy, T. E., Mason, K. O., Nousek, J. A., Ahr, L., Bingham, R. E., Broos, P. S., Carter, M. J., Hancock, B. K., Huckle, H. E., Hunsberger, S. D., Kawakami, H., Killough, R., Koch, T. S., McLelland, M. K., Smith, K., Smith, P. J., Soto, J. C., Boyd, P. T., Breeveld, A. A., Holland, S. T., Ivanushkina, M., Pryzby, M. S., Still, M. D., & Stock, J. 2005, *Space Science Reviews*, 120, 95
- Scaringi, S., Bird, A. J., Norton, A. J., Knigge, C., Hill, A. B., Clark, D. J., Dean, A. J., McBride, V. A., Barlow, E. J., Bassani, L., Bazzano, A., Fiocchi, M., & Landi, R. 2010, *MNRAS*, 401, 2207
- Scaringi, S., Connolly, S., Patterson, J., Thorstensen, J. R., Uthas, H., Knigge, C., Vican, L., Monard, B., Rea, R., Krajci, T., Lowther, S., Myers, G., Bolt, G., Dieball, A., & Groot, P. J. 2011, *A&A*, 530, A6+
- Smith, D. A. & Dhillon, V. S. 1998, *MNRAS*, 301, 767
- Southworth, J., Gänsicke, B. T., Marsh, T. R., de Martino, D., & Aungwerojwit, A. 2007a, *MNRAS*, 378, 635
- Southworth, J., Gänsicke, B. T., Marsh, T. R., de Martino, D., Hakala, P., Littlefair, S., Rodríguez-Gil, P., & Szkody, P. 2006, *MNRAS*, 373, 687
- Southworth, J., Marsh, T. R., Gänsicke, B. T., Aungwerojwit, A., Hakala, P., de Martino, D., & Lehto, H. 2007b, *MNRAS*, 382, 1145
- Thorstensen, J. R. 1986, *AJ*, 91, 940
- Walker, M. F. 1954, *PASP*, 66, 230
- . 1956, *ApJ*, 123, 68
- Warner, B. 1986, *MNRAS*, 219, 347

—. 1995, *Cataclysmic Variable Stars* (Cambridge: Cambridge University Press)

Warner, B. & Wickramasinghe, D. T. 1991, *MNRAS*, 248, 370

Warner, B. & Woudt, P. A. 2009, *MNRAS*, 397, 979

Witham, A. R., Knigge, C., Aungwerojwit, A., Drew, J. E., Gänsicke, B. T., Greimel, R., Groot, P. J., Roelofs, G. H. A., Steeghs, D., & Woudt, P. A. 2007, *MNRAS*, 382, 1158

Woudt, P. A. & Warner, B. 2003, *MNRAS*, 340, 1011

Wynn, G. A., King, A. R., & Horne, K. 1997, *MNRAS*, 286, 436

Zhang, E., Robinson, E. L., Stiening, R. F., & Horne, K. 1995, *ApJ*, 454, 447

Zorotovic, M., Schreiber, M. R., & Gänsicke, B. T. 2011, *A&A*, 536, A42

Table 1. Log of the observations, listing the date and UT of the observations, the exposure time, and the number of frames. All data were obtained in white light.

Date	UT	Exp.(s)	# Frames
2006 Dec 22	21:25-23:40	10-20	79
2006 Dec 23	20:58-06:37	5-10	372
2007 Oct 11	02:02-03:51	35	96
2007 Oct 14	01:59-06:23	35-45	225
2007 Oct 15	01:51-05:56	40	225
2007 Oct 16	01:53-06:04	45	210
2009 Nov 23	05:48-12:46	120	179

Table 2. The times of eclipse minima of IPHAS J0627.

Date	Eclipse minima (HJD)	Cycle	0–C (s)	References
2004 Nov 30	2453340.507625	0	13	Witham et al. (2007)
2004 Dec 02	2453342.548045	6	6	Witham et al. (2007)
2006 Dec 22	2454092.429208	2211	-36	this work
2006 Dec 23	2454093.449513	2214	-31	this work
2007 Oct 14	2454387.621588	3079	39	this work
2007 Oct 15	2454388.641673	3082	25	this work
2007 Oct 15	2454389.661442	3085	-16	this work
2009 Nov 23	2455158.929160	5347	50	this work



Table 3. Additional IPs with the respect to Fig. 23 of Gänsicke et al. (2005)

IPs	$P_{\text{orb}}$ (h)	$P_{\text{spin}}$ (s)	References
EIUMa	6.434	745.7	1,2
RX J2133+5107	7.193	570.82	3
SDSS J2333+1522	1.39	2499.6	4
IGR J0022+6141	4.033	563.53	5
IGR J19267+1325	4.58	938.6	6
IGR J15094-6649	5.89	808.7	7, 8
XSS J00564+4548 (= 1RXS J005528.0+461143)	2.568	470.1	8, 9, 10
V597 Pup	2.6687	261.9	11
IGR J16500-3307	3.617	571.9	7, 8
IGR J17195-4100	4.005	1062	7, 8
IRXS J165443.5-191620	3.7	546.66	12
IGR J08390-4833	8	1480.8	8
IGR J18308-1232	4.2	1820	8
IGR J18173-2509	6.6	831.7	8
IPHAS J0627	8.16	2210.27	this work

Note. — (1) In addition, we updated the spin periods of V2069 Cyg and 1RXS J0636+3535 to be  $P_{\text{spin}} =$

743.1 s and  $P_{\text{spin}} = 920$  s (Bernardini et al. 2012), respectively. (2) We did not include the confirmed IPs with uncertain  $P_{\text{orb}}$  determined e.g. SDSS J144659.95+025330.3 (Homer et al. 2006), Swift J0732-1331 (Butters et al. 2007), CXOPS J180354.3-300005 (Hong et al. 2009), AX J1740.2-2903 (Gotthelf & Halpern 2010), and IP candidates such as V426 Oph and LS Peg (Ramsay et al. 2008, and references therein).

References. — (1) Thorstensen (1986); (2) Reimer et al. (2008); (3) Bonnet-Bidaud et al. (2006); (4) Southworth et al. (2007a); (5) Bonnet-Bidaud et al. (2007); (6) Evans et al. (2008); (7) Pretorius (2009); (8) Bernardini et al. (2012); (9) Butters et al. (2008); (10) Bonnet-Bidaud et al. (2009); (11) Warner & Woudt (2009); (12) Scaringi et al. (2011)

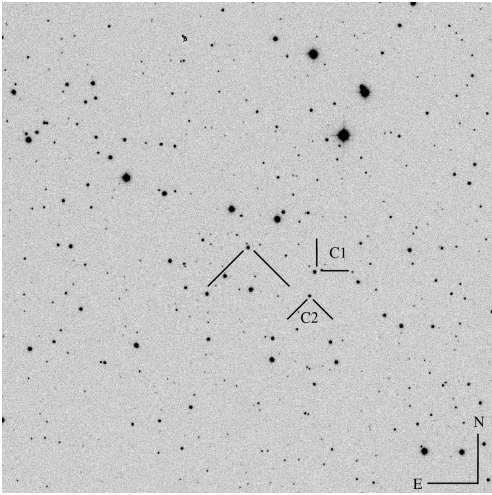


Fig. 1.— A  $7' \times 7'$  finding chart of IPHAS J0627 obtained from IPHAS imaging data. The J2000 coordinates of the star are  $\alpha = 06^{\text{h}}27^{\text{m}}46.4^{\text{s}}$  and  $\delta = +01^{\circ}48'11.1''$ . The comparison and check stars used in the photometry are marked by 'C1' and 'C2', respectively.

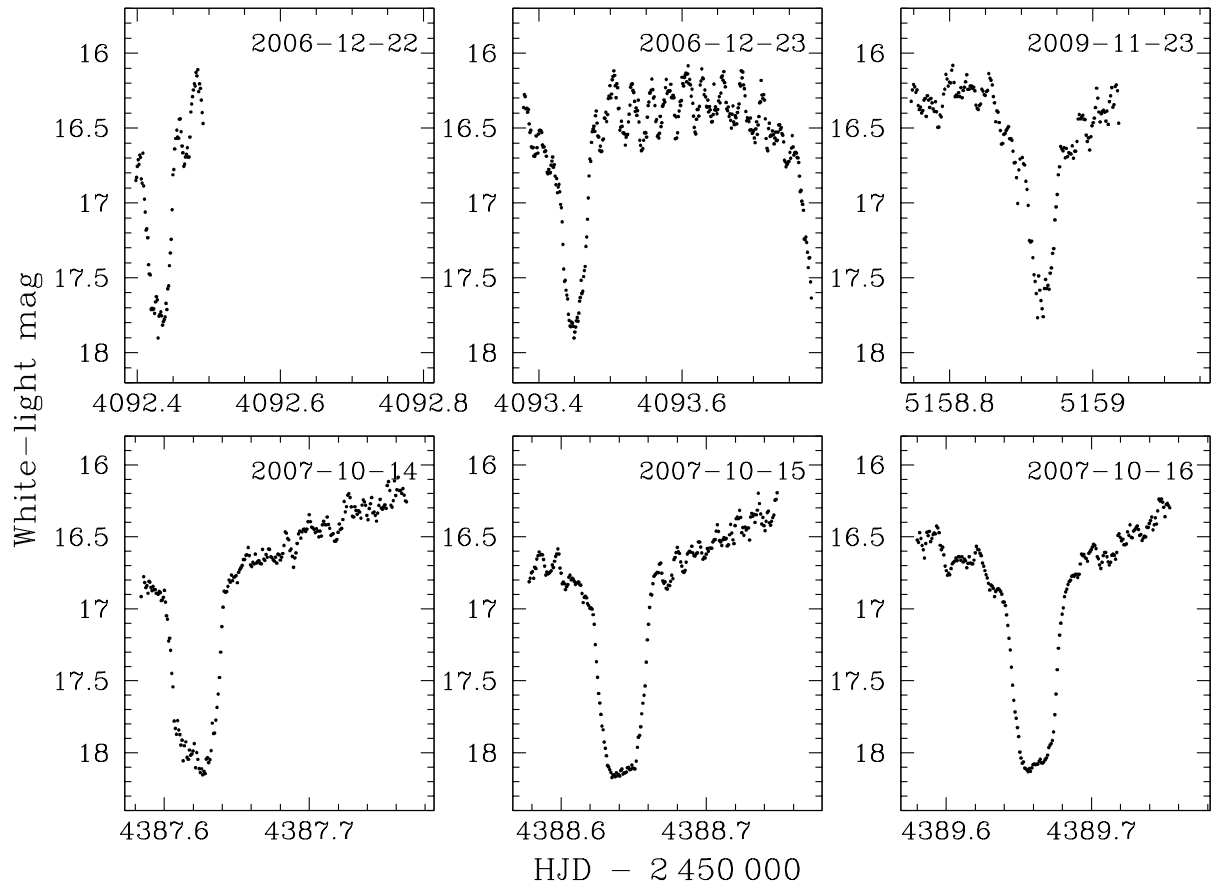


Fig. 2.— *Top*: 2006 and 2009 light curves of IPHAS J0627 show similar eclipse profile. *Bottom*: 2007 light curves reveal nightly variation in the eclipse profile.

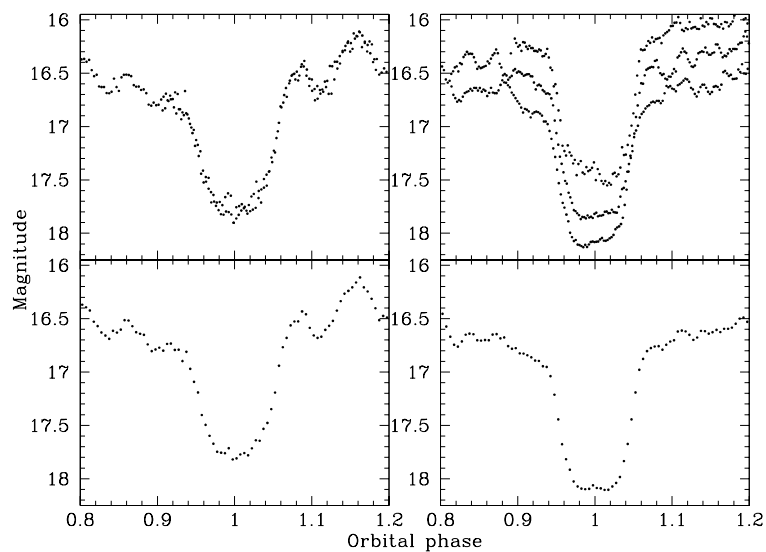


Fig. 3.— *Top*: the 2006 (left) and 2007 (right) eclipse profiles of IPHAS J0627 folded on the ephemeris in Eq. 1. The two eclipse observations from 2006 align very well in shape and depth. The 2007 October 14, 15, and 16 eclipses have been shifted by 0, -0.3, and -0.6 magnitudes to highlight the night-to-night variations in the eclipse profile. *Bottom*: the same data as in the top panels, but averaged into phase bins of  $\Delta\phi = 0.005$ .

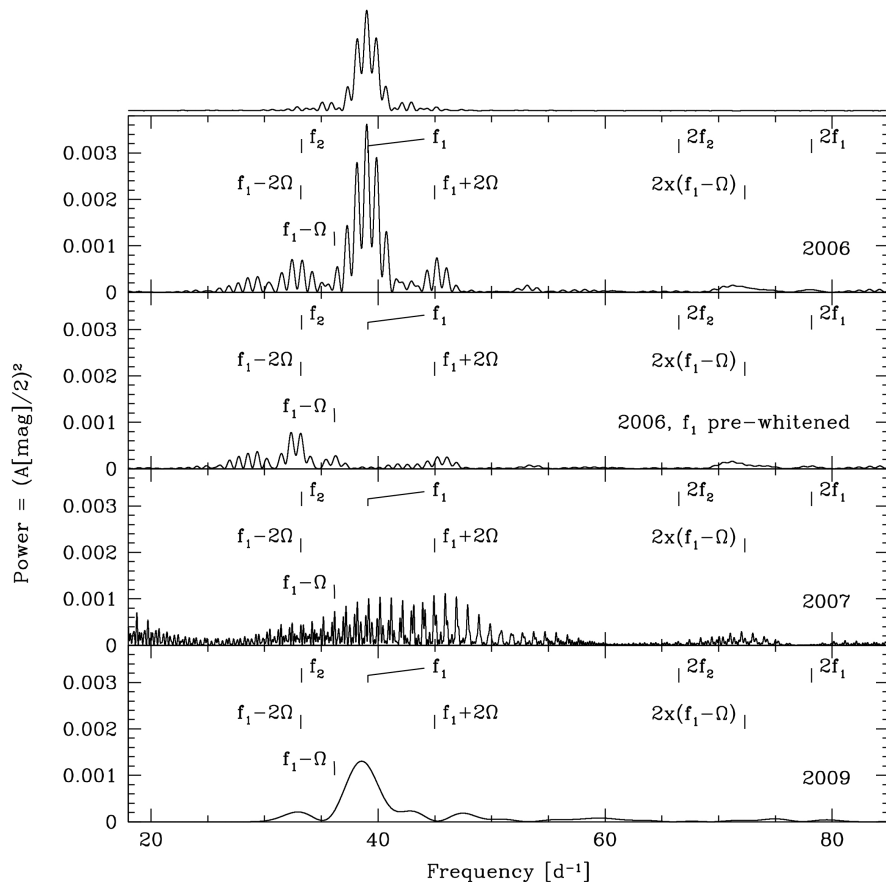


Fig. 4.— Power spectrum computed from the combined photometric data obtained in December 2006 (top panel), and the corresponding window function (above the figure). The power spectrum computed from the 2006 data after pre-whitening with the strongest signal,  $f_1 = 39.090(15) \text{ d}^{-1}$ , contains residual power at  $33.244(29) \text{ d}^{-1}$ , which, within the uncertainties is consistent with  $f_1 - 2\Omega$  (second panel). Additionally, there is some evidence for low-amplitude power near  $f_1 + 2\Omega$  and  $2(f_1 - \Omega)$ , whereas no signal is detected near the second harmonic of either  $f_1$  or  $f_2$ . The power spectra from October 2007 and November 2009 are shown in the third panel from the top, and the bottom panel, respectively.

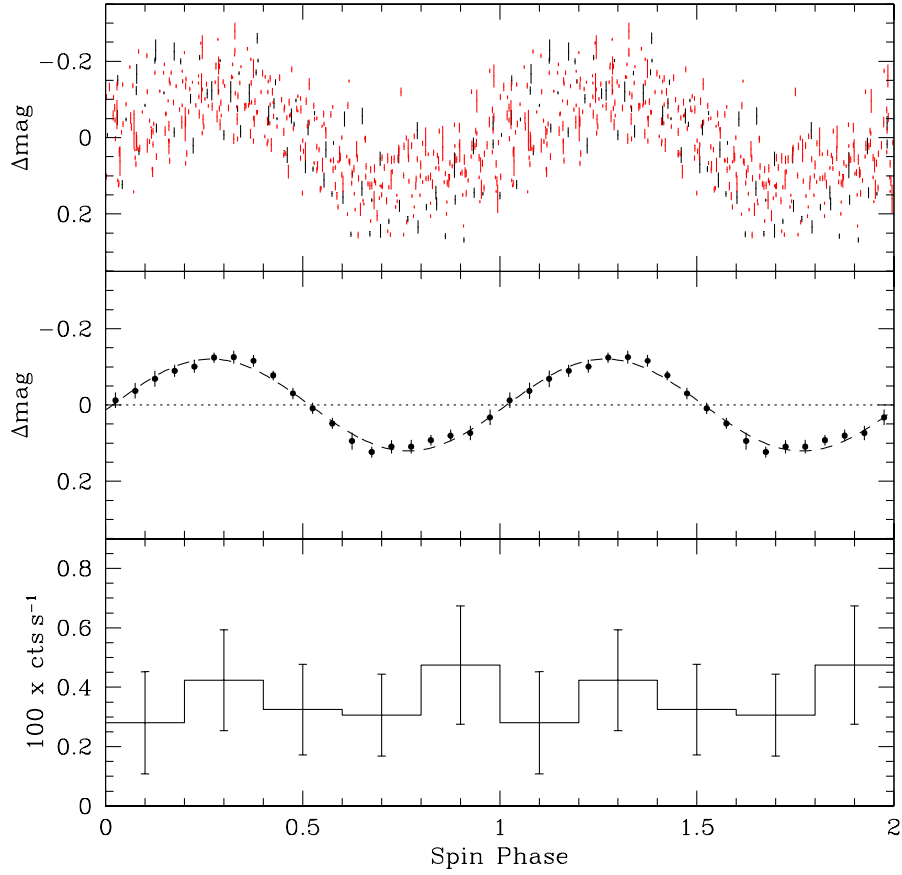


Fig. 5.— Spin-folded optical and X-ray light curve of IPHAS J0627 adopting  $P_{\text{spin}} = 2210$  s. The zero-point of the spin phase is arbitrary.

*Top:* all individual data points from December 2006 (black: December 22nd, red: December 23rd).

*Middle:* the 2006 data binned into 20 phase slots, along with a sine fit to the binned and folded data (dashed line).

*Bottom:* *Swift* XRT X-ray light curve of IPHAS J0627 folded on the spin period of 2210 s.

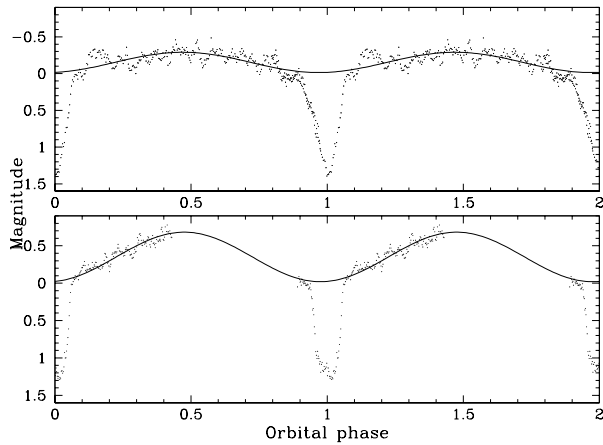


Fig. 6.— The orbital phase-folded light curves of IPHAS J0627 show a broad modulation, after pre-whitening with the adopted spin period of 2210 s for the 2006 data (*top panel*), and raw light curve for the 2007 data (*bottom panel*). Fitting this modulation with a sine results in amplitudes of the modulation of  $\sim 0.15$  mag in 2006 and  $\sim 0.33$  mag in 2007.

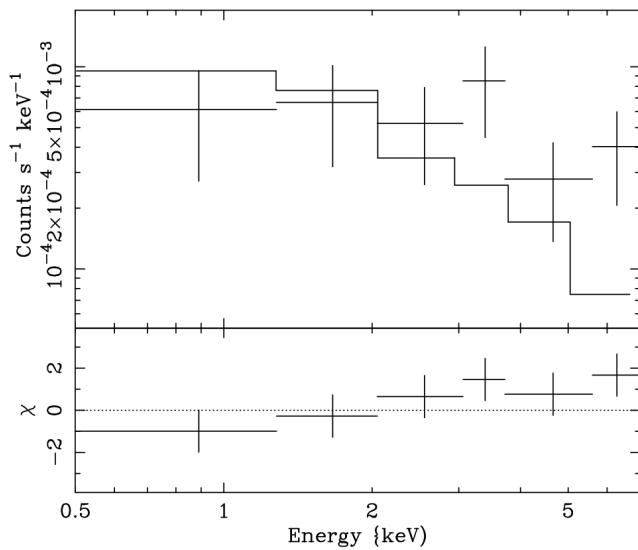


Fig. 7.— *Swift* XRT X-ray spectrum of IPHAS J0627. The model curve is an optically-thin thermal plasma model with temperature of 80 keV. The observed spectrum is harder than this model, indicating the presence of absorption that is well fit by a partial-covering absorber (see text).



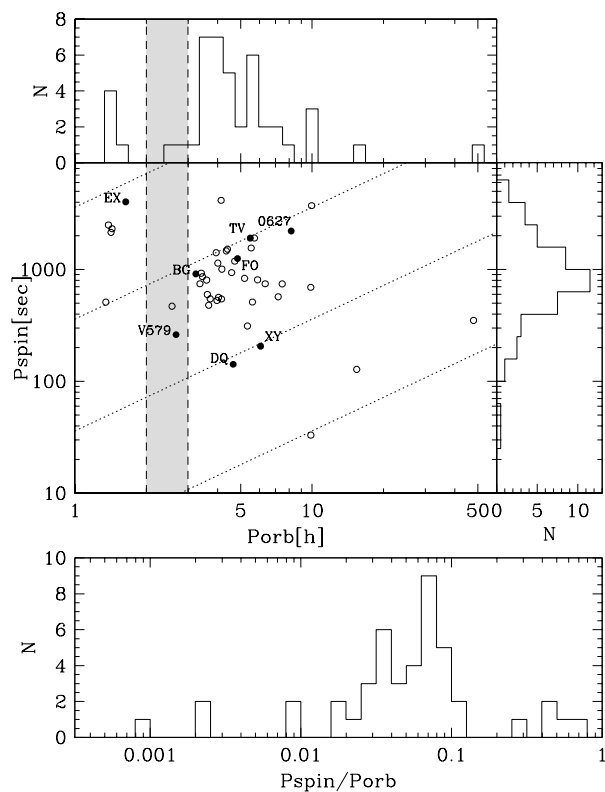


Fig. 8.— The updated period distribution of IPs on the original of Gänsicke et al. (2005). *Middle panel:* orbital and spin period of 48 IPs. The dotted lines indicate  $P_{spin}/P_{orb} = 1, 0.1, 0.01, 0.001$  from top to bottom, respectively. The eclipsing systems are shown as filled symbols. *Top panel:* orbital period distribution of the known IPs, the 2–3 h period gap is shaded grey. *Right panel:* spin period distribution of the known IPs.

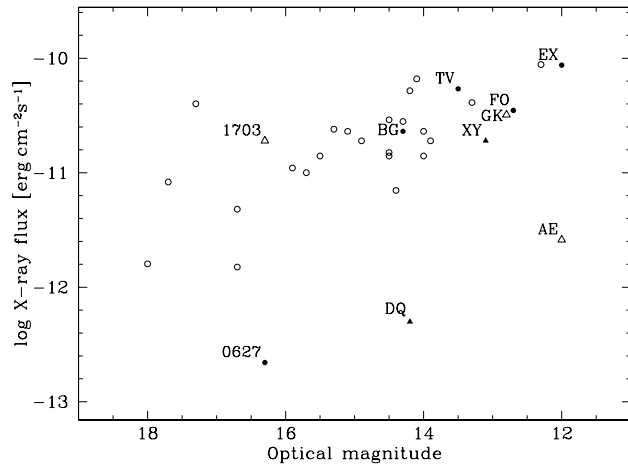


Fig. 9.— X-ray fluxes and optical magnitudes of the confirmed IPs. Filled dots represent eclipsing systems. Filled triangles are eclipsing and rapid rotators. Open triangles are rapid rotators.